Robust Position Control of a Tilt-Wing Quadrotor

C. Hancer, K. T. Oner, E. Sirimoglu, E. Cetinsoy, M. Unel

***Abstract*— This paper presents a robust position controller for a tilt-wing quadrotor to track desired trajectories under external wind and aerodynamic disturbances. Wind effects are modeled using Dryden model and are included in the dynamic model of the vehicle. Robust position control is achieved by introducing a disturbance observer which estimates the total disturbance acting on the system. In the design of the disturbance observer, the nonlinear terms which appear in the dynamics of the aerial vehicle are also treated as disturbances and included in the total disturbance. Utilization of the disturbance observer implies a linear model with nominal parameters. Since the resulting dynamics are linear, only PID type simple controllers are designed for position and attitude control. Simulations and experimental results show that the performance of the observer based position control system is quite satisfactory.**

I. INTRODUCTION

Autonomous unmanned aerial vehicles (UAV) are becoming increasingly capable nowadays and the complex mission tasks that are carried out by UAVs are far more critical than before. One of the basic tasks for an autonomously flying vehicle is to reach a desired location in space in an unsupervised manner because precise trajectory tracking is required to perform more complex missions in unconstrained environments. Recently significant interest in unmanned aerial vehicles directed researchers towards navigation problem of flying vehicles.

Most of the proposed solutions to the navigation problem are designed for outdoor operation, few techniques focus on indoor environments. In outdoor, GPS can be utilized for determination of the vehicle's position. In indoor applications, on the other hand, either GPS is not available or the accuracy of the measurements from GPS is not satisfactory.

Hoffmann et al. [1] propose a work related to attitude control algorithms. For position hold they use thrust vectoring with PID structure. In the work of Meister et al. [2], a sensor fusion algorithm for stable attitude and position estimation using GPS, IMU and compass modules together, is presented, and the control algorithms for position hold and waypoint tracking are developed. Hoffmann et al. [3] develop an autonomous trajectory tracking algorithm through cluttered environments for the STARMAC platform and a novel algorithm for dynamic trajectory generation. Puls et al. [4] presents the development of a position control system based on 2D GPS data for quadrotor vehicles. Using the proposed algorithm, the vehicle is able to keep positions above given destinations as well as to navigate between waypoints while minimizing trajectory errors. Waslander and Wang [5] focus on improvement of STARMAC quadrotor position hold performance by modeling the wind effects, i.e. using Dryden Wind Gust Model, on quadrotor dynamics in order to estimate wind velocities during fight. In [6], the main focus is on waypoint navigation, trajectory tracking, hovering and autonomous take-off and landing. An inexpensive Guidance Navigation and Control system is developed using low cost sensors.

In the literature there are also several works related to vision based navigation. For example, Soundararaj et al. [7] proposes a purely vision based navigation technique which relies on fast nearest neighbor classification for 3D localization and optical flow for velocity estimation. In the work of Azrad et al. [8], an object tracking system is used and the vision-control system enables the vehicle to track and hover above the target as long as the battery is available. Kendoul and his colleagues [9] present a visual navigation system based on pose estimation. In the work of Yu [10], an experimental study in hovering control of an unmanned helicopter with a 3D vision system instead of GPS is described.

In this work, we propose a robust position control system for the tilt-wing quadrotor aerial vehicle SUAVI (Sabanci University Unmanned Aerial VehIcle (see Figure 1). Dryden model is used to model wind gusts acting on the vehicle and these disturbances are included in the dynamic model of the vehicle. Thus, aerodynamic disturbances, which are not considered in many studies, are integrated into the system model. In order to estimate and compensate for the unknown disturbances, a "disturbance observer" [11] is utilized. This observer also takes into account the nonlinear terms in the dynamics of the vehicle and treats them as disturbances. As a result, a linear dynamical model with nominal parameters has been obtained. Since the disturbance observer provides robustness, only PID type controllers are employed to achieve robust positioning. The proposed observer based control approach is verified by simulations and experiments, and its performance has been found quite satisfactory.

Organization of the paper is as follows: Section II introduces the dynamic model of the vehicle including wind effects. Section III describes the design of the disturbance observer. Section IV is on flight controllers where position and attitude controllers are designed. Section V and VI are on simulation and experimental results, and related discussions. Finally, Section VII concludes the paper with some remarks and indicates possible future directions.

C. Hancer, K.T. Oner, E. Sirimoglu, E. Cetinsoy and M. Unel are with Sabanci University, Orhanli-Tuzla 34956, Istanbul TURKEY (corresponding author: munel@sabanciuniv.edu)

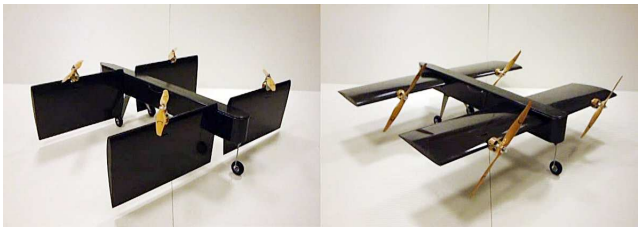

Fig. 1. SUAVI with integrated actuators in different flight configurations

II. DYNAMIC MODEL

In deriving dynamical models for unmanned aerial vehicles, it is usually preferred to express positional dynamics with respect to a fixed world coordinate frame and the rotational dynamics with respect to a body fixed frame attached to the vehicle. Making rigid body assumption, the dynamics of an unmanned aerial vehicle can be written as

$$\begin{bmatrix} mI_{3x3} & 0_{3x3} \\ 0_{3x3} & I_b \end{bmatrix} \begin{bmatrix} \dot{V}_w \\ \dot{\Omega}_b \end{bmatrix} + \begin{bmatrix} 0 \\ \Omega_b \times (I_b \Omega_b) \end{bmatrix} = \begin{bmatrix} F_t \\ M_t \end{bmatrix} \tag{1}$$

The subscripts w and b used in these equations express the vector and matrix quantities in world and body frames, respectively. V_w and Ω_b vectors represent the linear and the angular velocities of the vehicle with respect to the world and the body frames. m is the mass and I_b is the inertia matrix of the vehicle expressed in its body coordinate frame. I_{3x3} and 0_{3x3} matrices are 3×3 identity and zero matrices. Since the aerial vehicle is modeled as a 6 DOF rigid body, the left hand side of Equation (1) is standard for many aerial vehicles. Note that the total force and the moment, F_t and M_t, are platform dependent. We should remark that for a tilt-wing quadrotor these terms will be functions of the thrusts produced by the rotors and cosine and/or sine of the rotation angles of the wings (see [12] for details). Using vector-matrix notation above equations can be rewritten in a more compact form as

$$M\dot{\zeta} + C(\zeta)\zeta = G + O(\zeta)\omega + E(\xi)\omega^2 + W(\zeta) \tag{2}$$

where ζ denotes the vehicle's generalized velocity vector and is defined as

$$\zeta = [\dot{X}, \dot{Y}, \dot{Z}, p, q, r]^T \tag{3}$$

In (3), X, Y and Z are position coordinates of the center of mass of the vehicle with respect to the world frame, and p, q and r are angular velocities expressed in the body fixed frame. The vector ξ which appears in Equation (2), describes the position and the orientation of the vehicle with respect to the world frame, and is defined as

$$\xi = [X, Y, Z, \phi, \theta, \psi]^T \tag{4}$$

The mass-inertia matrix, M, the Coriolis-centripetal matrix, $C(\zeta)$, the gravity term, G, and the gyroscopic term are defined as

$$M = \begin{bmatrix} mI_{3x3} & 0_{3x3} \\ 0_{3x3} & diag(I_{xx}, I_{yy}, I_{zz}) \end{bmatrix} \tag{5}$$

$$C(\zeta) = \begin{bmatrix} 0 & 0 & 0 & 0 & 0 & 0 \\ 0 & 0 & 0 & 0 & 0 & 0 \\ 0 & 0 & 0 & 0 & 0 & 0 \\ 0 & 0 & 0 & 0 & I_{zz}r & -I_{yy}q \\ 0 & 0 & 0 & -I_{zz}r & 0 & I_{xx}p \\ 0 & 0 & 0 & I_{yy}q & -I_{xx}p & 0 \end{bmatrix} \tag{6}$$

$$G = [0, 0, mg, 0, 0, 0]^T \tag{7}$$

$$O(\zeta)\omega = J_{prop} \begin{pmatrix} 0_{3\times 1} \\ \sum_{i=1}^{4} J[\eta_i \Omega_b \times \begin{bmatrix} c_{\theta_i} \\ 0 \\ -s_{\theta_i} \end{bmatrix} \omega_i] \end{pmatrix} \tag{8}$$

where J_{prop} is the moment of inertia of the propeller about its rotation axis, $0_{3\times 1}$ is a 3×1 zero vector and ω_i is the propellers' speed.

System actuator vector, $E(\xi)\omega^2$, is defined as

$$E(\xi)\omega^2 = \begin{bmatrix} (c_\phi s_\theta c_\psi + s_\phi s_\psi)u_v + c_\psi c_\theta u_h \\ (c_\phi s_\theta s_\psi - s_\phi c_\psi)u_v + s_\psi c_\theta u_h \\ c_\phi c_\theta u_v - s_\theta u_h \\ (l_s s_{\theta_f} - c_{\theta_f}\lambda)u_{f_{dif}} + (l_s s_{\theta_r} + c_{\theta_r}\lambda)u_{r_{dif}} \\ [s_{\theta_f} u_{f_{sum}} - s_{\theta_r} u_{r_{sum}}]l_l \\ (l_s c_{\theta_f} + s_{\theta_f}\lambda)u_{f_{dif}} + (l_s c_{\theta_r} - s_{\theta_r}\lambda)u_{r_{dif}} \end{bmatrix} \tag{9}$$

$u_{(h,v,f_{dif},r_{dif},f_{sum},r_{sum})}$ terms used in Equation (9) are the horizontal, vertical, front differential, rear differential, front sum and rear sum thrust forces, respectively and they are defined as

$$u_{f_{sum}} = k(\omega_1^2 + \omega_2^2),\ u_{r_{sum}} = k(\omega_3^2 + \omega_4^2) \tag{10}$$

$$u_{f_{dif}} = k(\omega_1^2 - \omega_2^2),\ u_{r_{dif}} = k(\omega_3^2 - \omega_4^2) \tag{11}$$

$$u_v = -s_{\theta_f} u_{f_{sum}} - s_{\theta_r} u_{r_{sum}},\ u_h = c_{\theta_f} u_{f_{sum}} + c_{\theta_r} u_{r_{sum}} \tag{12}$$

where the following constraints are imposed on the wing angles, namely

$$\theta_f = \theta_1 = \theta_2,\ \theta_r = \theta_3 = \theta_4 \tag{13}$$

Parameters l_s and l_l denote distances between the rotors and the center of mass of the vehicle, and the parameters k and λ are lift and drag coefficients, respectively.

Lift and drag forces produced by the wings and the resulting moments due to these forces for different wing angles are defined as

$$W(\zeta) = \begin{bmatrix} R_{wb} \begin{bmatrix} F_D^1 + F_D^2 + F_D^3 + F_D^4 \\ 0 \\ F_L^1 + F_L^2 + F_L^3 + F_L^4 \end{bmatrix} \\ l_s(F_L^1 - F_L^2 + F_L^3 - F_L^4) \\ l_l(F_L^1 + F_L^2 - F_L^3 - F_L^4) \\ l_s(-F_D^1 + F_D^2 - F_D^3 + F_D^4) \end{bmatrix} \tag{14}$$

where R_{wb} is the rotation matrix between world and body coordinate axis, $F_D^i = F_D^i(\theta_i, v_x, v_z)$ and $F_L^i = F_L^i(\theta_i, v_x, v_z)$ are the lift and drag forces produced at the wings.

We should remark that above model boils down to a quadrotor model when $(\theta_{1,2,3,4} = \pi/2)$.

A. Modeling Wind Gusts

The effect of wind on quadrotor flight control can be significant and can lead to instabilities. In order to improve the positioning performance of the quadrotor, wind effects can be modeled and the generalized wind forces can be estimated. The wind estimate is used to reject the external disturbances created by the wind and gust effects.

The main framework of wind modeling represented in [5] depends on the Dryden wind-gust model. This model is defined as a summation of sinusoidal excitations:

$$v_\omega(t) = v_\omega^0 + \sum_{i=1}^{n} a_i sin(\Omega_i t + \varphi_i) \tag{15}$$

where $v_\omega(t)$ is a time dependent estimate of the wind vector given time t, randomly selected frequencies Ω_i in the range of 0.1 to 1.5 rad/s and phase shifts φ_i. n is the number of sinusoids, a_i is the amplitude of sinusoids and v_ω^0 is the static wind vector. The magnitudes a_i are defined as $a_i = \sqrt{\Delta\Omega_i \Phi(\Omega_i)}$ where $\Delta\Omega_i$ are frequency intervals between different frequencies and $\Phi(\Omega_i)$ are the power spectral densities. The power spectral density for vertical and horizontal winds are different and can be determined from the following equations:

$$\Phi_h(\Omega) = \sigma_h^2 \frac{2L_h}{\pi} \frac{1}{1+(L_h\Omega)^2} \tag{16}$$

$$\Phi_v(\Omega) = \sigma_v^2 \frac{2L_v}{\pi} \frac{1+3(L_v\Omega)^2}{(1+(L_v\Omega)^2)^2} \tag{17}$$

Here σ_h and σ_v are horizontal and vertical turbulence intensities respectively. L_h and L_v are horizontal and vertical gust length scales. It is stated that these relations are valid for altitudes below 1000 feet [5]. The relations between L_h and L_v, and σ_h and σ_v are altitude dependent as can be seen from the following equations:

$$\frac{L_h}{L_v} = \frac{1}{(0.177+0.000823Z)^{1.2}} \tag{18}$$

$$\frac{\sigma_h}{\sigma_v} = \frac{1}{(0.177+0.000823Z)^{0.4}} \tag{19}$$

Using velocities predicted by this wind model, generalized forces are calculated by multiplying wind velocities by related aerodynamic drag coefficients. These generalized forces are integrated into the dynamic model given in Eq. (2) as external disturbances $D(\zeta,\xi)$. After incorporating the external disturbances, the final form of the dynamic model of the quadrotor vehicle given in Eq. (20) becomes as follows:

$$M\dot{\zeta} + C(\zeta)\zeta = G + O(\zeta)\omega + E(\xi)\omega^2 + W(\zeta) + D(\zeta,\xi) \tag{20}$$

III. DISTURBANCE OBSERVER

In this section, we design a disturbance observer [11], which is frequently used in motion control systems, to estimate the total disturbance acting on the system. In addition to the external disturbances, nonlinear terms and parametric uncertainties are also included in the total disturbance.

We first note that the mass-inertia matrix of the aerial vehicle can be written as $M = M_{nom} + \tilde{M}$. Here, M_{nom} refers to the nominal inertia matrix with nominal mass and inertia parameters, and $(\tilde{M})$ is the difference between actual and nominal mass-inertia matrices.

Equation (20) can be rewritten in terms of the nominal inertia matrix explicitly as

$$M_{nom}\dot{\zeta} = f + \tau_{dist} \tag{21}$$

where f and τ_{dist} are the actuator input and and the total disturbance, respectively, and are defined as

$$f = E(\xi)\omega^2$$

$$\tau_{dist} = -\tilde{M}\dot{\zeta} - C(\zeta)\zeta + G + O(\zeta)\Omega + W(\zeta) + D(\zeta,\xi) \tag{22}$$

Note that τ_{dist} contains, in addition to the external disturbances like wind and gust, the nonlinear terms and the parametric uncertainties in the dynamics.

Equation (21) can be rewritten as 6 scalar equations of the form

$$M_{nom_i}\dot{\zeta}_i = f_i + \tau_{dist_i}, \quad i = 1,\ldots,6 \tag{23}$$

Taking the Laplace transform and solving for τ_{dist_i} imply

$$\tau_{dist_i}(s) = M_{nom_i} s\zeta_i(s) - f_i(s) \tag{24}$$

In order to estimate the disturbance given by (24), both sides of the equation can be multiplied by $G(s) = \frac{g}{s+g}$, i.e. transfer function of a low-pass filter, to obtain

$$G(s)\tau_{dist_i}(s) = M_{nom_i} sG(s)\zeta_i(s) - G(s)f_i(s) \tag{25}$$

Note that, $sG(s)$ can be written as

$$sG(s) = s\frac{g}{s+g} = g(1-\frac{g}{s+g}) = g(1-G(s)) \tag{26}$$

Let's define the term $G(s)\tau_{dist_i}(s)$ by $\hat{\tau}_{dist_i}(s)$, i.e. estimated disturbance. Thus,

$$\hat{\tau}_{dist_i}(s) = -G(s)f_i(s) - gM_{nom_i}G(s)\zeta_i(s) + gM_{nom_i}\zeta_i(s) \tag{27}$$

Subtracting the estimated disturbance from the control input, i.e. $f_i \leftarrow f_i - \hat{\tau}_{dist_i}$, we obtain

$$M_{nom_i} s\zeta_i(s) = f_i(s) + (1-G(s))\tau_{dist_i}(s) \tag{28}$$

Note that due to low-pass filter $G(s) \approx 1$ in the low frequency range. Thus, for low frequencies the total disturbance on the system is eliminated and the input-output description of the system becomes a linear model with nominal parameters, namely

$$M_{nom_i}\dot{\zeta}_i = f_i \tag{29}$$

The block diagram of the implemented disturbance observer is depicted in 2.

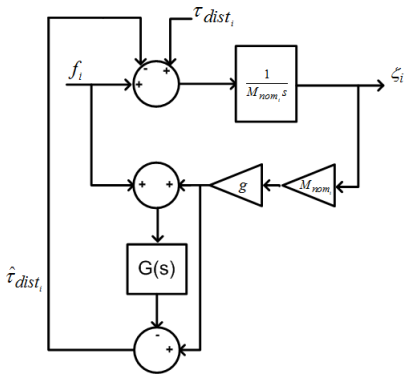

Fig. 2. Block diagram of the disturbance observer

IV. FLIGHT CONTROLLERS

A. Position Controllers

In order to develop flight controllers, we will follow the approach detailed in [3]. A path, P $\in$ NxR^3 is generated by N waypoints $\mathbf{x}_i^d$. Let the desired flight speeds of the vehicle between two consecutive waypoints i and $i+1$ be v_i^d. For each path segment P_i, the vehicle travels along the subpath vector that combines $\mathbf{x}_i^d$ and $\mathbf{x}_{i+1}^d$. A unit tangent vector $\mathbf{t}_i$ and a unit normal vector $\mathbf{n}_i$ along and perpendicular to the subpath vector are defined. Let $x(t)$ be the current position of the vehicle measured from GPS. The cross track error e_{ct} and its derivative, and along track error rate $\dot{e}_{at}$ are defined as

$$e_{ct} = (\mathbf{x}_i^d - \mathbf{x}(t)) \cdot \mathbf{n}_i \tag{30}$$

$$\dot{e}_{ct} = -\mathbf{v}(t) \cdot \mathbf{n}_i \tag{31}$$

$$\dot{e}_{at} = v_i^d - \mathbf{v}(t) \cdot \mathbf{t}_i \tag{32}$$

As proposed in [3], a PI controller is designed for the along track direction and a PID controller is designed for the cross track direction; i.e.

$$u_{at} = K_{atp}\dot{e}_{at} + K_{ati}\int_0^t \dot{e}_{at}dt \tag{33}$$

$$u_{ct} = K_{ctp}e_{ct} + K_{ctd}\dot{e}_{ct} + K_{cti}\int_0^t e_{ct}dt \tag{34}$$

Desired acceleration vector in XY plane of the vehicle is constructed from the controller outputs (33) and (34) as,

$$a_{des} = R(\psi)(u_{ct} \cdot \mathbf{n} + u_{at} \cdot \mathbf{t}) \tag{35}$$

where $R(\psi)$ is a 2D rotation matrix which performs the necessary transformation of the acceleration using the heading (ψ) of the vehicle.

The reference attitude angles of the vehicle that enable the vehicle to travel in the desired trajectory is obtained from the desired acceleration vector as follows:

$$\theta_{ref} = -\arcsin(\frac{a_x}{||a||}) \tag{36}$$

$$\phi_{ref} = \arcsin(\frac{a_y}{||a||\cos(\theta)}) \tag{37}$$

In these equations, a refers to the linear acceleration of the aerial vehicle, $a = (a_x, a_y, a_z)$, a_x and a_y are x and y components of the acceleration vector defined in (35) respectively. The third component of the acceleration vector a_z is the acceleration of the vehicle along z axis which is computed as $a_z = u_1/m$. Note that θ is the instantaneous pitch angle measured by IMU. $||.||$ symbol refers to Euclidean norm and for the acceleration vector a it is defined as

$$||a|| = \sqrt{a_x^2 + a_y^2 + a_z^2} \tag{38}$$

Reference values computed using Equations (36) and (37) should be filtered by a low-pass filter in order to be used by the attitude controller.

B. Altitude and Attitude Controllers

In order to develop altitude and attitude controllers, we first recall the quadrotor's altitude (Z) and attitude (ϕ, θ and ψ) dynamics; i.e.

$$\ddot{Z} = -c_\theta c_\phi \frac{u_1}{m} + g$$

$$\dot{p} = \frac{u_2}{I_{xx}} + \frac{I_{yy} - I_{zz}}{I_{xx}}qr - \frac{J}{I_{xx}}q\omega_p$$

$$\dot{q} = \frac{u_3}{I_{yy}} + \frac{I_{zz} - I_{xx}}{I_{yy}}pr + \frac{J}{I_{yy}}p\omega_p$$

$$\dot{r} = \frac{u_4}{I_{zz}} + \frac{I_{xx} - I_{yy}}{I_{zz}}pq + \frac{u_4}{I_{zz}} \tag{39}$$

where $\omega_p = \omega_1 - \omega_2 - \omega_3 + \omega_4$ is the total propeller speed.

For controller design, attitude dynamics can be linearized around hover conditions, i.e. $\phi \approx 0$, $\theta \approx 0$ and $\psi \approx 0$, where angular accelerations in body and world frames can be assumed to be approximately equal, i.e. $\dot{p} \approx \ddot{\phi}$, $\dot{q} \approx \ddot{\theta}$, $\dot{r} \approx \ddot{\psi}$. Resulting altitude and attitude dynamics can be expressed as

$$\ddot{Z} = -(c_\theta c_\phi)\frac{u_1}{m} + g,\ \ddot{\phi} = \frac{u_2}{I_{xx}},\ \ddot{\psi} = \frac{u_4}{I_{zz}},\ \ddot{\theta} = \frac{u_3}{I_{yy}} \tag{40}$$

Altitude and attitude controllers are then designed by the following expressions:

$$u_1 = K_{p,z}e_z + K_{d,z}\dot{e}_z + K_{i,z}\int e_z dt - \frac{mg}{c_\theta c_\phi}$$

$$u_2 = K_{p,\phi}e_\phi + K_{d,\phi}\dot{e}_\phi + K_{i,\phi}\int e_\phi dt$$

$$u_3 = K_{p,\theta}e_\theta + K_{d,\theta}\dot{e}_\theta + K_{i,\theta}\int e_\theta dt$$

$$u_4 = K_{p,\psi}e_\psi + K_{d,\psi}\dot{e}_\psi + K_{i,\psi}\int e_\psi dt \tag{41}$$

where $e_q = q^d - q$ for $q = Z, \phi, \theta, \psi$. Note that the altitude controller given by the first equation in (41) is a gravity compensated PID controller. Similarly, other three orientation controllers are also PID controllers. In these controllers $K_{p,q} > 0$, $K_{d,q} > 0$ and $K_{i,q} > 0$ are proportional, derivative and integral control gains, respectively.

V. SIMULATION RESULTS

Two simulation results will be presented in this section. In the first one, the 3D cartesian reference trajectory is an elliptical helix shown in Figure 3 where the actual trajectory followed by the aerial vehicle is also superimposed. Attitude angles and position coordinates are depicted in Figures 4 and 5 along with references. Note that reference angles and positions are tracked with reasonably small tracking errors. As seen in the figures, aerial vehicle tracks the reference attitude angles (ϕ_{ref} and θ_{ref}), obtained from desired cartesian acceleration vector via Equations (36) and (37), very accurately with an error of less than $\pm 2^o$. Moreover, heading of the vehicle is also kept around zero with an error less than $\pm 1^o$.

To see if the generated thrusts by the rotors remain within physical limits, which is 16 N, rotor forces are plotted in Figure 6. Clearly they are kept within the physical limits. One might wonder what kind of wind forces acted on the system. They are shown in Figure 7. The estimation and compensation of the disturbance acting on the aerial vehicle is quite important for trajectory tracking performance. The components of the total disturbance estimated by the disturbance observer are depicted in Figure 8. Note that these components are similar to components of the wind and gust forces plotted in Figure 7, which are the dominant component of the total disturbance.

In the second simulation, a 2D cartesian trajectory (square) is tracked by the aerial vehicle. Figure 9 depicts the result of this simulation. As in the previous simulation, the trajectory tracking performance of the proposed observer based control system is quite satisfactory.

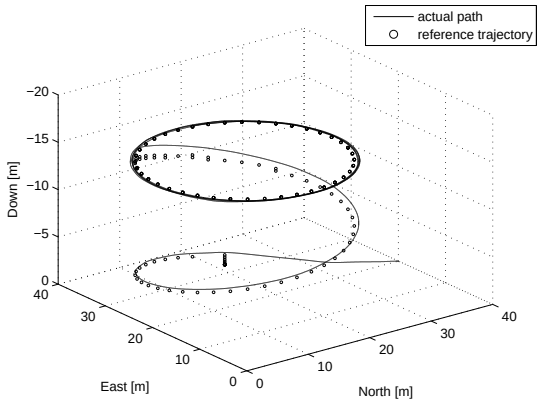

Fig. 3. Elliptical helix shaped trajectory tracking performance

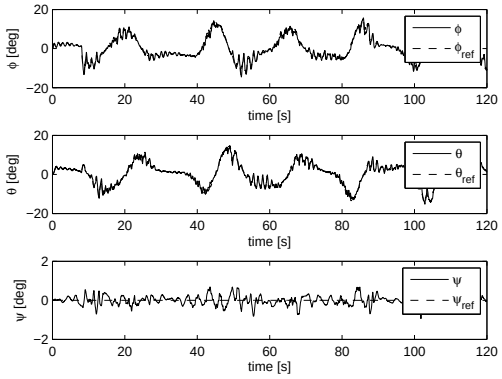

Fig. 4. Attitude tracking performance

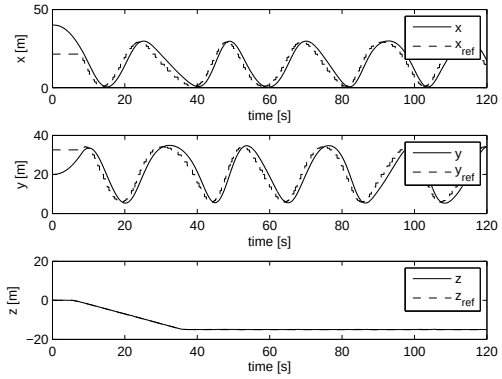

Fig. 5. Position tracking performance

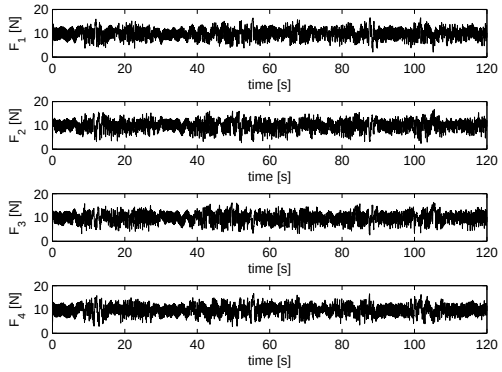

Fig. 6. Thrust forces created by rotors

VI. EXPERIMENTAL RESULTS

To see the effectiveness of the proposed method in real flight tests, several hovering experiments are performed. In outdoor conditions where wind effects are present, the aerial vehicle is successfully hovered around a point using the disturbance observer based control system. Results are depicted in Figures 10. The proposed hovering controller is implemented in the onboard microprocessor of the vehicle. Note that the aerial vehicle takes off from a reference position, hovers in the neighborhood of this reference position and lands successfully.

VII. CONCLUSIONS AND FUTURE WORKS

In this paper, a robust position controller for a tilt-wing quadrotor for way-points tracking under external wind and aerodynamic disturbances are presented. Robustness of the controller is achieved by employing a disturbance observer

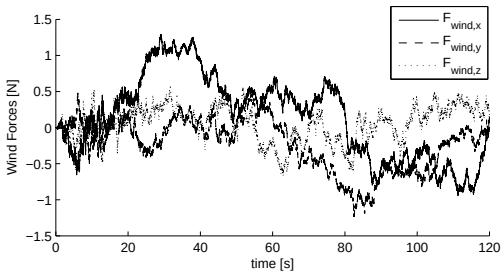

Fig. 7. Wind forces acting as disturbance

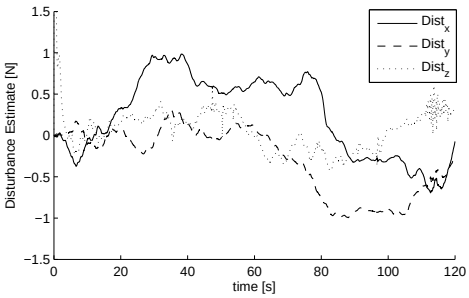

Fig. 8. Disturbance Estimation

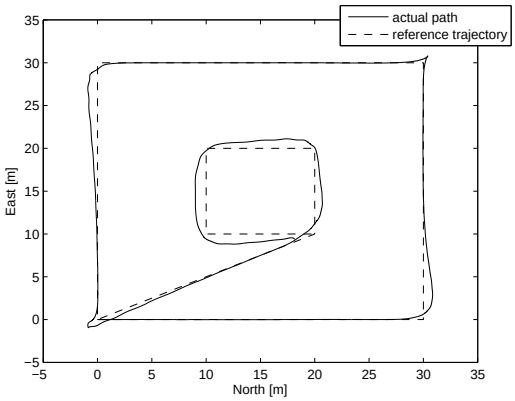

Fig. 9. Square shaped trajectory tracking performance

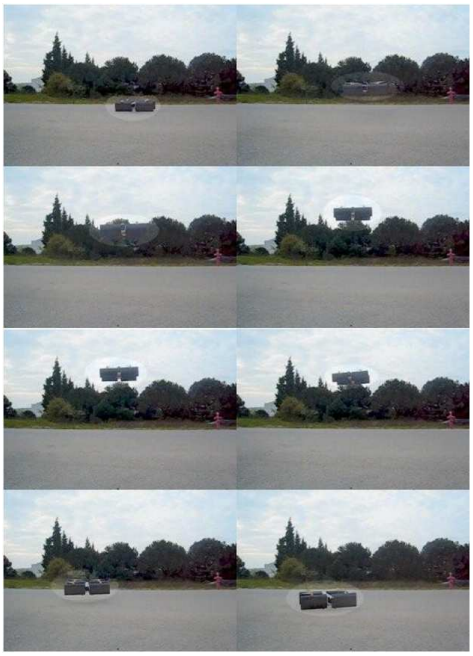

Fig. 10. Hovering of aerial vehicle in outdoor environment

which estimates the total disturbance acting on the system and compensates for it. Trajectory tracking performance of the vehicle is tested via simulations in Matlab/Simulink and satisfactory performance is obtained using this controller. Furthermore, performance of the hovering controller is verified with experiments. Future works include implementation of the trajectory tracking algorithm on our tilt-wing aerial vehicle SUAVI.

VIII. ACKNOWLEDGMENTS

Authors would like to acknowledge the support provided by TUBITAK under grant 107M179.

REFERENCES

[1] Gabriel M. Hoffmann, Haomiao Huang, Steven L. Waslander, and Claire J. Tomlin, "Quadrotor helicopter flight dynamics and control: Theory and experiment", In Proceedings of the AIAA Guidance, Navigation and Control Conference and Exhibit, Hilton Head, South Carolina, August, 2007.

[2] O. Meister, R. Mnikes, J. Wendel, N. Frietsch, C. Schlaile, G. F. Trommer, "Development of a GPS/INS/MAG navigation system and waypoint navigator for a VTOL UAV", ISPIE Unmanned Systems Technology IX, Orlando, FL, USA, April 9-12, 2007, vol. 6561, p. 65611D (2007)

[3] G. M. Hoffmann, S. L Waslander, and C. J. Tomlin, "Quadrotor helicopter trajectory tracking control", In 2008 AIAA Guidance, Navigation and Control Conference and Exhibit, Honolulu, Hawaii, USA, August 2008.

[4] T. Puls, M. Kemper, R. Kke, A. Hein, "GPS Based Position Control and Waypoint Navigation System for Quadrocopters", IEEE/RSJ International Conference on Intelligent Robots and Systems, October 11-15, 2009, St. Louis, MO, USA. IEEE 2009.

[5] Steven L. Waslander and Carlos Wang, "Wind disturbance estimation and rejection for quadrotor position control", In AIAA Infotech@Aerospace Conference and AIAA Unmanned...Unlimited Conference, Seattle, WA, April 2009.

[6] F. Kendoul, Y. Zhenyu, K. Nonami, "Embedded Autopilot for Accurate Waypoint Navigation and Trajectory Tracking", Application to Miniature Rotorcraft UAVs (2009 IEEE International Conference on Robotics and Automation Kobe, Japan, May 12-17, 2009)

[7] S. Soundararaj, A. Sujeeth, "Autonomous Indoor Helicopter Flight Using a Single Onboard Camera", Proceedings of the IEEE International Conference on Intelligent Robots and System, St. Luis, USA, October 11-15 (2009)

[8] S. Azrad, F.Kendoul, D.Perbrianti and K. Nonami, "Visual Servoing of an Autonomous Micro Air Vehicle for Ground Object Tracking Syaril", Proceedings of the IEEE International Conference on Intelligent Robots and System, St. Luis, USA, October 11-15 (2009)

[9] F.Kendoul, K. Nonami, "A Visual Navigation System for Autonomous Flight of Micro Air Vehicle", Proceedings of the IEEE International Conference on Intelligent Robots and System, St. Luis, USA, October 11-15 (2009)

[10] Z. Yu, L. Tang, "Experiment in 3D Vision Based Hovering Control of an Autonomous Helicopter", Journal of System Design and Dynamics, Volume 1, Issue 2, pp. 120-128 (2007)

[11] K. Ohnishi, T. Murakami, "Advanced Motion Control in Robotics", IEEE, IECON, vol.2, pp.356- 359, 1989.

[12] K. T. Oner, E. Cetinsoy, E. Sirimoglu, C. Hancer, T. Ayken, M. Unel, "LQR and SMC Stabilization of a New Unmanned Aerial Vehicle", Proceedings of International Conference on Intelligent Control, Robotics, and Automation (ICICRA 2009), Venice, Italy, October 28-30, 2009.